

# Descriptor Distillation: a Teacher-Student-Regularized Framework for Learning Local Descriptors

Yuzhen Liu<sup>1,2</sup> and Qiulei Dong<sup>1,2\*</sup>

<sup>1</sup>State Key Laboratory of Multimodal Artificial Intelligence Systems, CASIA, Beijing, 100190, China.

<sup>2</sup>School of Artificial Intelligence, UCAS, Beijing, 100049, China.

\*Corresponding author(s). E-mail(s): [qldong@nlpr.ia.ac.cn](mailto:qldong@nlpr.ia.ac.cn);  
Contributing authors: [liuyuzhen22@mails.ucas.ac.cn](mailto:liuyuzhen22@mails.ucas.ac.cn);

## Abstract

Learning a fast and discriminative patch descriptor is a challenging topic in computer vision. Recently, many existing works focus on training various descriptor learning networks by minimizing a triplet loss (or its variants), which is expected to decrease the distance between each positive pair and increase the distance between each negative pair. However, such an expectation has to be lowered due to the non-perfect convergence of network optimizer to a local solution. Addressing this problem and the open computational speed problem, we propose a *Descriptor Distillation* framework for local descriptor learning, called DesDis, where a student model gains knowledge from a pre-trained teacher model, and it is further enhanced via a designed teacher-student regularizer. This teacher-student regularizer is to constrain the difference between the positive (also negative) pair similarity from the teacher model and that from the student model, and we theoretically prove that a more effective student model could be trained by minimizing a weighted combination of the triplet loss and this regularizer, than its teacher which is trained by minimizing the triplet loss singly. Under the proposed DesDis, many existing descriptor networks could be embedded as the teacher model, and accordingly, both equal-weight and light-weight student models could be derived, which outperform their teacher in either accuracy or speed. Experimental results on 3 public datasets demonstrate that the equal-weight student models, derived from the proposed DesDis framework by utilizing three typical descriptor learning networks as teacher models, could achieve significantly better performances than their teachers and several other comparative methods. In addition, the derived light-weight models could achieve 8 times or even faster speeds than the comparative methods under similar patch verification performances.

**Keywords:** local descriptor, knowledge distillation, deep learning

## 1 Introduction

Local descriptor learning plays an important role in various visual tasks, such as image retrieval (Ng et al., 2020, Noh et al., 2017), panorama stitching (Brown and Lowe, 2007, Herrmann et al., 2018), structure-from-motion (Dong et al., 2020,

Schonberger and Frahm, 2016) and multi-view stereo (Radénović et al., 2016, Schönberger et al., 2016). The existing descriptors in literature could be roughly divided into two categories: hand-crafted descriptors and learning-based descriptors. Early works (Bay et al., 2008, Dong and Soatto, 2015, Lowe, 2004) mainly focused on hand-crafted

ones according to researchers' expertise. Recently, learning-based descriptors (Balntas et al., 2016, Bökman and Kahl, 2022, Dusmanu et al., 2021, 2019, Ke and Sukthankar, 2004, Luo et al., 2018, Mishchuk et al., 2017, Pautrat et al., 2020, Revaud et al., 2019, Sun et al., 2021, Tian et al., 2020, 2019, Zhao et al., 2022), particularly DNN(Deep Neural Network)-based descriptors, have shown a significant priority to their hand-crafted counterparts. A comprehensive overview could be found in (Ma et al., 2021).

Different from the hand-crafted descriptors, DNN-based descriptors are automatically learned via deep neural networks, which are trained by utilizing large-scale local patch datasets (Balntas et al., 2020, Brown et al., 2010) with ground truth correspondences. In recent years, a lot of descriptor learning networks have employed a triplet loss (Balntas et al., 2016, Mishchuk et al., 2017) or its variants (Tian et al., 2020, 2019), that are expected to enforce the distances of positive pairs of patch descriptors to be smaller while the distances of negative pairs to be larger. However, due to the complexity of these descriptor learning networks, their used optimizers generally converge to local minima at the training stage (Faghri et al., 2018, Wang et al., 2017, Yu et al., 2018) (this is to say, the distances of the positive pairs of descriptors learned by these networks are not sufficiently smaller, while the distances of the negative pairs of descriptors learned by these networks are not sufficiently larger), resulting in lower-than-expected performances.

In order to alleviate the above local convergence problem and additionally speed up the descriptor inference, we propose a *Descriptor Distillation* framework for local descriptor learning, called DesDis, which is inspired by the model compression ability of the knowledge distillation technique in some other visual tasks, such as image classification (Hinton et al., 2015, Zhuang et al., 2022), object detection (Huang et al., 2020, Ma et al., 2022) and face recognition (Huang et al., 2022, Low et al., 2021). It has to be pointed out that knowledge distillation is originally a model compression technique, which aims to transfer knowledge from a pre-trained teacher model to a smaller student model, but it is not deliberately designed for improving model accuracy. Hence, under the proposed framework, given

a teacher model (which could be an arbitrary existing descriptor learning network), a teacher-student regularizer is firstly designed to alleviate the aforementioned local convergence problem and enhance the ability of the student model by minimizing the difference between the positive (also negative) pair similarity under the teacher model and that under the student model. Then, we prove theoretically in Section 3.4 that by minimizing a weighted combination of the triplet loss and the designed regularizer, the distances of positive (or negative) descriptor pairs from the student model could be smaller (or larger) than those from its teacher model. Consequently, different student models with different compression rates for learning either more discriminative or faster local descriptors could be naturally derived under the proposed DesDis framework by utilizing different existing descriptor learning networks as teacher models.

In sum, our main contributions include:

- We propose the DesDis framework for local descriptor learning through knowledge distillation, where many existing descriptor learning networks could be seamlessly embedded as the teacher models.
- We explore the teacher-student regularizer under the proposed DesDis framework, which is helpful to further decrease (or increase) the distances of positive (or negative) pairs of descriptors output by the student model in comparison to the teacher model at the training stage. In addition, we give a theoretical proof of the effectiveness of this regularizer.
- Given an arbitrary teacher model under the proposed DesDis framework, not only a more discriminative equal-weight student model, but also a set of light-weight student models that achieve a trade-off between computational accuracy and speed, could be derived, whose effectiveness has been demonstrated by the experimental results in Section 4.

The rest of the paper is organized as follows. Section 2 gives a review on DNN-based local descriptors and knowledge distillation in other visual tasks. Section 3 introduces the framework in detail. Experimental results are reported in Section 4. Section 5 concludes the paper.

## 2 Related Work

Here, we firstly review some DNN-based methods for descriptor learning in literature. Then, considering that the proposed framework employs the knowledge distillation technique, we also give a review on knowledge-distillation-based methods for handling other visual tasks.

### 2.1 DNN-based Local Descriptors

As discussed in Section 1, in recent years, DNN-based methods for descriptor learning have shown a significant priority to the early hand-crafted methods (Bay et al., 2008, Dong and Soatto, 2015, Ke and Sukthankar, 2004, Lowe, 2004) in literature. MatchNet (Han et al., 2015) employed a siamese architecture, where one branch was used for mapping a patch to a feature representation and the other was used for measuring the similarity of features. Balntas et al. (2016) used a triplet margin loss with anchor swap to construct triplets. Tian et al. (2017) proposed the L2Net for learning local descriptors, which utilized a fully convolutional architecture. Mishchuk et al. (2017) adopted the ‘hardest in the batch’ strategy to sample negative pairs. He et al. (2018) directly optimized a ranking-based retrieval performance metric for learning local descriptors. Luo et al. (2018) integrated the geometric constraints from multi-view reconstructions, which could benefit the learning process in terms of data generalization, data sampling and loss computation. Tian et al. (2019) jointly used the traditional first order similarity loss term and a designed second order similarity regularizer to train a descriptor network. Tian et al. (2020) showed theoretically and empirically that a hybrid similarity measure could balance the gradients from negative and positive samples. In addition, unlike (Balntas et al., 2016, He et al., 2018, Mishchuk et al., 2017, Tian et al., 2020, 2019) where a large number of local image patches are used as inputs for network training, some works (Dusmanu et al., 2019, Luo et al., 2020, Revaud et al., 2019, Tyszkiewicz et al., 2020) also investigated to use whole images as input for training and then output the descriptors of all the key points together in each input image.

It is worth noting that the aforementioned works (Balntas et al., 2016, He et al., 2018, Luo et al., 2018, Mishchuk et al., 2017, Tian

et al., 2020, 2017, 2019) aimed to train descriptor learning networks with a set of local patches by simultaneously minimizing the distances of positive descriptor pairs and maximizing the distances of negative descriptor pairs with a triplet loss or its variants, but these works were prone to obtaining local solutions in practice due to the networks’ complexity. This issue motivates us to design a more effective regularizer (i.e. the teacher-student regularizer which would be described in detail in Section 3.2), which could ensure that the distances of positive descriptor pairs would be further decreased while those of negative descriptor pairs would be further increased in both theory and practice.

### 2.2 Knowledge Distillation in Other Visual Tasks

Knowledge distillation is a model compression technique, where a student network is trained to mimic a pre-trained teacher model. The student model could benefit from extra supervisory signal by the soft information from the teacher network. It was firstly proposed for image classification by Hinton et al. (2015). Following this seminal work, the knowledge distillation technique has been extended to handle different visual tasks, such as object detection (Huang et al., 2020, Ma et al., 2022), face recognition (Huang et al., 2022, Low et al., 2021), image segmentation (He et al., 2019, Hou et al., 2020), pose estimation (Nie et al., 2019, Zhang et al., 2018), etc. For example, Ma et al. (2022) explored a knowledge distillation method to transfer the knowledge of unseen categories for object detection. Huang et al. (2022) proposed an evaluation-oriented knowledge distillation method for deep face recognition, which could reduce the performance gap between the teacher and student models during training. Zhang et al. (2018) proposed a fast pose distillation model training method enabling to more effectively train small human pose CNN networks.

Here, the following two points have to be explained:

- (i) It is noted that Lee et al. (2021) introduced the concept of ‘feature distillation’ for descriptor learning, which is to directly learn a descriptor from the features extracted from the intermediate layers of a pretrained convolutional network,

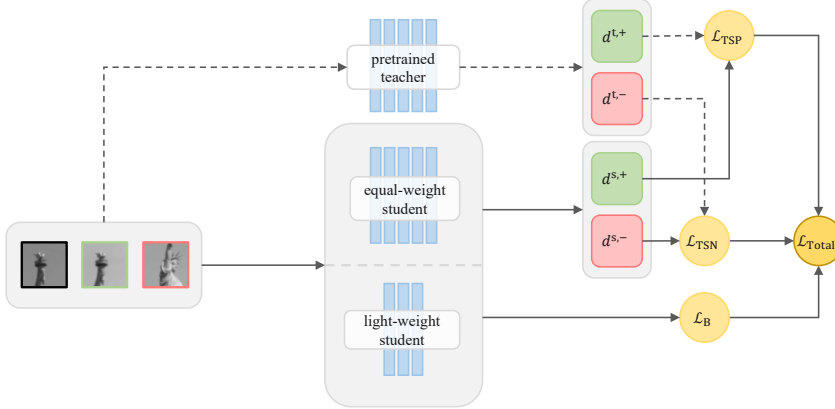


**Fig. 1** The pipeline of the proposed DesDis framework.  $d^{t,+}$  and  $d^{t,-}$  are the distances of positive and negative descriptor pairs from the teacher model.  $d^{s,+}$  and  $d^{s,-}$  are the distances of positive and negative descriptor pairs from the student model.  $\mathcal{L}_B$  is a triplet loss variant.  $\mathcal{L}_{TSP}$  and  $\mathcal{L}_{TSN}$  are the two forms of the teacher-student regularizer.

and it is significantly different from the concept of knowledge distillation used in our work and the aforementioned works (Hinton et al., 2015, Luo et al., 2016, Ma et al., 2022, Nie et al., 2019), which is to pursue a student model from a given teacher model.

- (ii) As discussed above, knowledge distillation is originally a model compression technique, but it is not deliberately designed for improving model accuracy. Hence, although the original knowledge distillation technique (Hinton et al., 2015) is seemingly able to be used for handling the descriptor learning task, it is intrinsically unable to guarantee a student model with a higher accuracy, even with a comparable accuracy to its teacher model. This is the issue that also motivates us to explore the teacher-student regularizer in the following section.

### 3 Methodology

In this section, we propose the DesDis framework with the designed teacher-student regularizer for local descriptor learning. Firstly, we describe the pipeline of the DesDis framework. Then, we present the teacher-student regularizer as well as the total loss function. Finally, we give a theoretical analysis on the designed teacher-student regularizer.

#### 3.1 The DesDis Framework

The proposed DesDis framework utilizes a knowledge distillation strategy, whose pipeline is shown in Fig. 1. As seen from this figure, the DesDis

framework consists of a pre-trained teacher model, a student model, and a loss function for training the student model. In principle, many existing networks (Balntas et al., 2016, He et al., 2018, Mishchuk et al., 2017, Tian et al., 2020, 2017) for descriptor learning could be straightforwardly used as teacher models, and the goal of DesDis is to pursue such a student model that could not only gain knowledge from the pre-trained teacher model, but also achieve better performances by introducing a teacher-student regularizer.

In this work, we use or design the following two kinds of student models:

- (i) **Equal-weight student model:** For a pre-trained teacher model, we straightforwardly adopt its architecture as the corresponding equal-weight student model.
- (ii) **Light-weight student model:** Here, a light-weight student model means a smaller model with fewer parameters than a given teacher model. Considering that the number of the convolutional layers in many state-of-the-art descriptor networks (Mishchuk et al., 2017, Tian et al., 2020, 2017, 2019) are no less than 7, we design a set of 5-convolutional-layer networks with different numbers of channels as light-weight student models, whose architecture is shown in Fig. 2. These models are denoted as DesDis- $D$ , where  $D$  represents the channel number in the first convolutional layer, and is set to  $\{8, 16, 24, 32\}$  respectively in our work.

In the following parts, we will describe the designed teacher-student regularizer as well as the

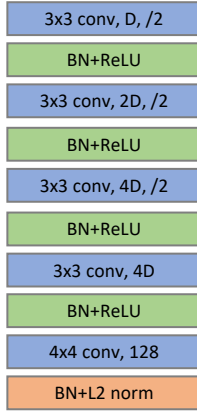


**Fig. 2** Architectures of the design light-weight model DesDis-D which consists of 5 convolutional layers. ‘\2’ denotes strided convolution with a stride of 2.

total loss function  $\mathcal{L}_{\text{Total}}$  in detail, and provide the theoretical analysis on the designed teacher-student regularizer.

### 3.2 Teacher-Student Regularizer

As discussed in Section 1, many existing descriptor learning methods (Balntas et al., 2016, Mishchuk et al., 2017, Tian et al., 2020, 2017, 2019) are trained by minimizing the triplet loss or its variants, and the distances of the positive (or negative) pairs of their learned descriptors are not sufficiently smaller (or larger). This issue motivates us to design the following teacher-student (TS) regularizer under the proposed descriptor distillation framework consisting of a pretrained teacher model, which could be one of the aforementioned works (Balntas et al., 2016, Mishchuk et al., 2017, Tian et al., 2020, 2017, 2019), and a student model, so that the distances of positive descriptor pairs are further decreased and the distances of negative descriptor pairs are increased in the student model, comparing with the pre-trained teacher model. The proposed TS regularizer neither maximizes the similarity of each positive pair nor minimizes the similarity of each negative pair, but it aims to minimize the difference between the positive (also negative) pair similarity from the teacher model and that from the student model.

Specifically, given  $N$  anchor sample patches,  $N$  matching patches and  $N$  non-matching patches, their corresponding descriptors learned by the teacher model are denoted as  $\{x_i^t\}_{i=1}^N$ ,  $\{x_i^{t,+}\}_{i=1}^N$  and  $\{x_i^{t,-}\}_{i=1}^N$  respectively, and similarly, their corresponding descriptors learned by the student

model are denoted as  $\{x_i^s\}_{i=1}^N$ ,  $\{x_i^{s,+}\}_{i=1}^N$  and  $\{x_i^{s,-}\}_{i=1}^N$  respectively. The TS regularizer has dual forms for handling positive and negative pairs respectively. The form for positive pairs is formulated as:

$$\mathcal{L}_{\text{TSP}} = \frac{1}{N} \sum_{i=1}^N (d_i^{t,+} - d_i^{s,+})^2 \quad (1)$$

where  $d_i^{t,+} = \|x_i^t - x_i^{t,+}\|_2$ ,  $d_i^{s,+} = \|x_i^s - x_i^{s,+}\|_2$  are the Euclidean distances of the  $i$ -th positive pair of descriptors learned by the teacher and student models respectively (‘ $\|\cdot\|_2$ ’ denotes the  $L_2$  norm).

Similarly, the form of the TS regularizer for negative pairs is formulated as:

$$\mathcal{L}_{\text{TSN}} = \frac{1}{N} \sum_{i=1}^N (d_i^{t,-} - d_i^{s,-})^2 \quad (2)$$

where  $d_i^{t,-} = \|x_i^t - x_i^{t,-}\|_2$ ,  $d_i^{s,-} = \|x_i^s - x_i^{s,-}\|_2$  are the Euclidean distances of the  $i$ -th negative pair of descriptors learned by the teacher and student models respectively.

### 3.3 Total Loss Function

It is noted from Eqn. (1) and Eqn. (2) that the designed TS regularizer requires neither each positive pair to be closer, nor each negative pair to be more distant. Hence, this regularizer is not used singly for training the student model under the proposed DesDis framework. Instead, it is used jointly with the triplet-like loss term  $\mathcal{L}_B$  of the pre-trained teacher model.

In this work, the total loss function  $\mathcal{L}_{\text{Total}}$  for training the student model is a weighted combination of the loss term  $\mathcal{L}_B$  of the teacher model and the two aforementioned dual forms of the TS regularizer as:

$$\mathcal{L}_{\text{Total}} = \mathcal{L}_B + \alpha_p \mathcal{L}_{\text{TSP}} + \alpha_n \mathcal{L}_{\text{TSN}} \quad (3)$$

where  $\alpha_p$  and  $\alpha_n$  are two preset weight parameters.  $\mathcal{L}_B$  could be the classic triplet loss or its variants in the existing works (Mishchuk et al., 2017, Tian et al., 2020, 2019).

### 3.4 Theoretical Analysis

In this subsection, we give a theoretical proof that once the regularizer is used, the distances of

positive (or negative) pairs of descriptors in the student model are smaller (or larger) than those in the teacher model at the training stage.

Here, we analyze the fundamental case where the classic triplet loss  $\mathcal{L}_T$  in Eqn. (4) is used as the loss term  $\mathcal{L}_B$  in the total loss function (3).

The classic triplet loss  $\mathcal{L}_T$  is formulated as:

$$\mathcal{L}_T = \frac{1}{N} \sum_{i=1}^N \max(0, m + d_i^+ - d_i^-) \quad (4)$$

where  $m$  is a hyperparameter.

For a pre-trained teacher model which has been trained by minimizing the triplet loss  $\mathcal{L}_T$ , the distances  $\{d_i^{t,+}\}_{i=1}^N$  of  $N$  positive descriptor pairs and the distances  $\{d_i^{t,-}\}_{i=1}^N$  of  $N$  negative descriptor pairs in the teacher model could be straightforwardly obtained. Then, we give the following proposition on the student model which is trained by minimizing the total loss function (3) with  $\mathcal{L}_T$ :

**Proposition 1** *Given the distances  $\{d_i^{t,+}\}_{i=1}^N$  of  $N$  positive descriptor pairs and the distances  $\{d_i^{t,-}\}_{i=1}^N$  of  $N$  negative descriptor pairs in the teacher model, under the condition that  $m + d_i^{s,+} - d_i^{s,-} > 0, i = 1, 2, \dots, N$ , the optimal solution to the total loss function (3) with  $\mathcal{L}_T$  satisfies:*

$$d_i^{s,+} < d_i^{t,+}, \quad d_i^{s,-} > d_i^{t,-}, \quad i = 1, 2, \dots, N$$

*Proof* By replacing  $\mathcal{L}_B$  in Eqn. (3) with the triplet loss  $\mathcal{L}_T$  in 4, under the condition that  $m + d_i^{s,+} - d_i^{s,-} > 0, i = 1, 2, \dots, N$ , the total loss function could be re-formulated as:

$$\begin{aligned} \mathcal{L}_{\text{Total}} &= \frac{1}{N} \sum_{i=1}^N [\max(0, m + d_i^{s,+} - d_i^{s,-}) + \\ &\quad \alpha_p(d_i^{t,+} - d_i^{s,+})^2 + \alpha_n(d_i^{t,-} - d_i^{s,-})^2] \\ &= \frac{1}{N} \sum_{i=1}^N [(m + d_i^{s,+} - d_i^{s,-}) + \\ &\quad \alpha_p(d_i^{t,+} - d_i^{s,+})^2 + \alpha_n(d_i^{t,-} - d_i^{s,-})^2] \end{aligned} \quad (5)$$

$\mathcal{L}_{\text{Total}}$  is a convex function of  $d_i^{s,+}$  and  $d_i^{s,-}, i = 1, 2, \dots, N$ , hence its optimal solution is achieved if and only if its first-order derivatives with respect to both  $d_i^{s,+}$  and  $d_i^{s,-}$  are equal to zero.

The first-order partial derivatives of  $\mathcal{L}_{\text{Total}}$  with respect to  $d_i^{s,+}$  and  $d_i^{s,-}$  are:

$$\begin{aligned} \frac{\partial \mathcal{L}_{\text{Total}}}{\partial d_i^{s,+}} &= 1 + 2\alpha_p d_i^{s,+} - 2\alpha_p d_i^{t,+} \\ \frac{\partial \mathcal{L}_{\text{Total}}}{\partial d_i^{s,-}} &= -1 + 2\alpha_n d_i^{s,-} - 2\alpha_n d_i^{t,-} \end{aligned} \quad (6)$$

Accordingly, by letting both  $\frac{\partial \mathcal{L}_{\text{Total}}}{\partial d_i^{s,+}}$  and  $\frac{\partial \mathcal{L}_{\text{Total}}}{\partial d_i^{s,-}}$  in Eqn. (6) to be 0, we obtain:

$$\begin{aligned} d_i^{s,+} &= d_i^{t,+} - \frac{1}{2\alpha_p} \\ d_i^{s,-} &= d_i^{t,-} + \frac{1}{2\alpha_n} \end{aligned} \quad (7)$$

Since  $\frac{1}{2\alpha_p}$  and  $\frac{1}{2\alpha_n}$  are two positive numbers, it holds:

$$d_i^{s,+} < d_i^{t,+}, \quad d_i^{s,-} > d_i^{t,-}, \quad i = 1, 2, \dots, N$$

□

Proposition 1 reveals that given a pre-trained teacher model, the distances of positive descriptor pairs in the student model which is trained by jointly minimizing the triplet loss and the designed regularizer are smaller than those in the teacher model at the training stage in theory, while the distances of negative descriptor pairs in the student model are larger than those in the teacher model.

It is also noted that Proposition 1 holds true under the condition that ' $m + d_i^{s,+} - d_i^{s,-} > 0$ ' ( $i = 1, 2, \dots, N$ ), and this condition could be met with a high probability when  $m$  is set to be a large constant. Here, we also conduct the following experiment to empirically analyze this condition: We train HardNet (Mishchuk et al., 2017) (a typical local descriptor network which is trained by minimizing the classic triplet loss where the margin is set to be  $m = 1$ ) on the Liberty subset of Brown and derive the corresponding equal-weight student model DesDis-HardNet accordingly. Then, we randomly sample 100K triplets from the Liberty subset of Brown, and 100K triplets from the HPatches dataset (Baltntas et al., 2020) respectively, by following the hard negative mining strategy used in HardNet. The corresponding  $\{m + d_i^{s,+} - d_i^{s,-}\}_{i=1}^{100000}$  from the student model DesDis-HardNet are obtained, and the distributions are shown in Fig. 3a and Fig. 3b. As seen from the two figure, the condition ' $m + d_i^{s,+} - d_i^{s,-} > 0$ ' ( $i = 1, 2, \dots, N$ ) holds true in most cases on both the Brown and

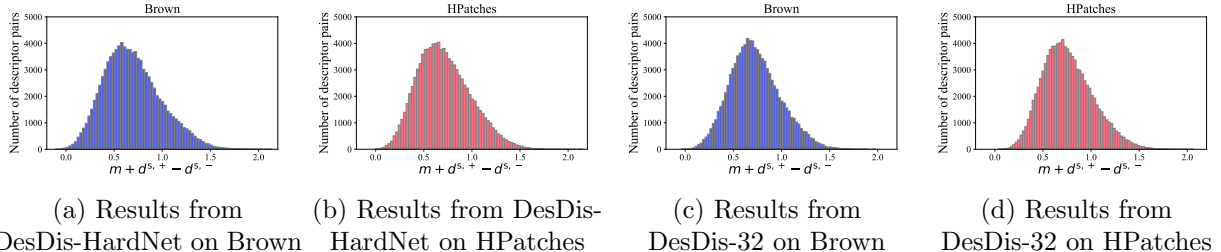


**Fig. 3** The distribution of (a) ‘ $m + d^{s,+} - d^{s,-}$ ’ from DesDis-HardNet on Brown, (b) ‘ $m + d^{s,+} - d^{s,-}$ ’ from DesDis-HardNet on HPatches, (c) ‘ $m + d^{s,+} - d^{s,-}$ ’ from DesDis-32 (using SIFT as teacher) on Brown, and (d) ‘ $m + d^{s,+} - d^{s,-}$ ’ from DesDis-32 (using SIFT as teacher) on HPatches. ‘ $d^{s,+}$ ’ and ‘ $d^{s,-}$ ’ denote the distance of positive and negative pairs respectively from the student.

HPatches datasets. In fact, less than 100 of 100K samples do not meet this condition on the two datasets, this is to say, this condition could be met with more than 99.9% probability. Moreover, we use the typical handcrafted descriptor SIFT (Lowe, 2004) as the teacher and train the student model DesDis-32 on the Liberty subset of Brown under the proposed framework. The corresponding  $\{m + d_i^{s,+} - d_i^{s,-}\}_{i=1}^{100000}$  on Brown and HPatches are shown in Fig. 3c and Fig. 3d respectively. As seen from the two figures, the condition could also be met with a high probability.

## 4 Experimental Results

In this section, we first describe the used three public datasets and the comparison group. Then, we introduce the implementation details. Next, we evaluate both the equal-weight and light-weight student models derived from the proposed DesDis framework on the three public datasets. Finally, the ablation study is provided.

### 4.1 Datasets and Comparison Group

**Datasets:** In this paper, we use three public datasets for evaluating our method, including the Brown dataset (Brown et al., 2010), the HPatches dataset (Balntas et al., 2020) and the ETH SfM dataset (Schönberger et al., 2017).

The Brown dataset (Brown et al., 2010) is the most widely used patch dataset for evaluating the patch verification performance of local descriptors. It consists of three subsets: *Liberty*, *Notredame* and *Yosemite*. The test set consists of 100K matching and non-matching pairs for each sequence.

The HPatches dataset (Balntas et al., 2020) consists of over 1.5 million patches extracted from 116 viewpoint and illumination changing scenes. According to the geometric noise levels, the extracted patches are classified into the *easy*, *hard*, and *tough* groups respectively. Three tasks are performed on the three groups of patches, including patch verification, image matching, and patch retrieval.

The ETH benchmark (Schönberger et al., 2017) is designed for image-based 3D reconstruction. We follow the setup in (Tian et al., 2020, 2019), *i.e.*, all learning-based methods are trained on the *Liberty* subset of Brown (Brown et al., 2010). Since the patches used in the comparative methods are not given in the original papers (Tian et al., 2020, 2019), we extract the patches using the DoG detector, and use these patches for all the methods.

**Comparison Group:** As indicated in Section 1, under the proposed DesDis framework, not only a more discriminative equal-weight student model, but also a set of light-weight student models that achieve a trade-off between computational accuracy and speed could be derived. Accordingly, the comparative evaluation is divided into two groups: In Section 4.3, we evaluate the equal-weight student models derived under the proposed DesDis framework. In Section 4.4, we evaluate the light-weight student models.

### 4.2 Implementation Details

In the equal-weight student model scenario, we firstly train the teacher models by implementing the code released by Tian et al. (2020, 2019) for 200 epochs with the learning rate of 0.01 and

**Table 1** Comparative evaluation on the Brown dataset (Brown et al., 2010). The numbers in the seven columns on the right are false positive rate at 95% recall. The best results are in **bold**. ‘DesDis-’ denotes the derived student model trained under the proposed DesDis framework. ‘†’ denotes the baseline models that are trained without the proposed teacher-student regularizer. The throughputs are evaluated on a GTX 1650Ti GPU.

Train	#Param.	Throughputs	ND		LIB		LIB		Mean
			LIB	YOS	ND	YOS	LIB	ND	
Test		(K patch/sec)	Equal-Weight						
SIFT	-	-	29.84		22.53		27.29		26.55
MatchNet	-	-	7.04	11.47	3.82	5.65	11.6	8.70	8.05
TFeat	0.60M	100	7.39	10.13	3.06	3.80	8.06	7.24	6.64
L2Net	1.33M	17	2.36	4.70	0.72	1.29	2.57	1.71	2.22
DOAP	1.33M	17	1.54	2.62	0.43	0.87	2.00	1.21	1.45
Light-Weight									
HardNet	1.33M	17	1.49	2.51	0.53	0.78	1.96	1.84	1.51
DesDis-HardNet	1.33M	17	<b>1.31</b>	<b>2.03</b>	<b>0.48</b>	<b>0.72</b>	<b>1.54</b>	<b>1.31</b>	<b>1.23</b>
SOSNet	1.33M	17	1.08	2.12	<b>0.35</b>	0.67	1.03	0.95	1.03
DesDis-SOSNet	1.33M	17	<b>1.02</b>	<b>1.91</b>	0.36	<b>0.60</b>	<b>0.96</b>	<b>0.82</b>	<b>0.95</b>
HyNet	1.34M	12	0.89	<b>1.37</b>	0.34	0.61	0.88	0.96	0.84
DesDis-HyNet	1.34M	12	<b>0.86</b>	<b>1.37</b>	<b>0.29</b>	<b>0.48</b>	<b>0.70</b>	<b>0.60</b>	<b>0.71</b>
Light-Weight									
DesDis-8 <sup>†</sup>	0.08M	440	4.06	5.61	1.69	1.88	4.96	3.74	3.66
DesDis-8	0.08M	440	<b>3.95</b>	<b>5.23</b>	<b>1.46</b>	<b>1.68</b>	<b>4.69</b>	<b>3.71</b>	<b>3.45</b>
DesDis-16 <sup>†</sup>	0.19M	294	<b>2.35</b>	3.77	0.77	1.13	2.97	2.18	2.20
DesDis-16	0.19M	294	2.37	<b>3.15</b>	<b>0.72</b>	<b>1.05</b>	<b>2.59</b>	<b>2.06</b>	<b>1.99</b>
DesDis-24 <sup>†</sup>	0.33M	183	2.04	2.96	0.63	0.96	2.06	1.73	1.73
DesDis-24	0.33M	183	<b>1.91</b>	<b>2.69</b>	<b>0.59</b>	<b>0.88</b>	<b>1.87</b>	<b>1.69</b>	<b>1.61</b>
DesDis-32 <sup>†</sup>	0.50M	145	1.81	2.86	0.55	0.90	2.01	1.69	1.64
DesDis-32	0.50M	145	<b>1.52</b>	<b>2.36</b>	<b>0.54</b>	<b>0.81</b>	<b>1.68</b>	<b>1.48</b>	<b>1.39</b>

the batch size of 1024. We use Adam optimizer with  $\alpha = 0.01$ ,  $\beta_1 = 0.9$  and  $\beta_2 = 0.999$ . Then, the trained teacher models are used for deriving the corresponding student models under the proposed framework. We set the weights  $\alpha_p$  and  $\alpha_n$  in Eqn. (3) to 1 and 15 respectively.

In the light-weight student model scenario, both  $\alpha_p$  and  $\alpha_n$  are set to 9. The models are trained for 200 epochs with the learning rate of 0.01 and Adam optimizer. We adopt HyNet (Tian et al., 2020) as the teacher model for all the light-weight student models.

### 4.3 Equal-Weight Student Models Under DesDis

In this subsection, we use three typical local descriptor learning networks HardNet (Mishchuk et al., 2017), SOSNet (Tian et al., 2019), HyNet (Tian et al., 2020) as the teacher models under the proposed DesDis framework, and derive the

corresponding equal-weight students, denoted as DesDis-HardNet, DesDis-SOSNet, DesDis-HyNet.

#### 4.3.1 Evaluation on Brown

We evaluate the derived three equal-weight student models in comparison to their teacher models and 6 additional state-of-the-arts methods, including SIFT (Lowe, 2004), DeepDesc (Simo-Serra et al., 2015), MatchNet (Han et al., 2015), TFeat (Balntas et al., 2016), L2Net (Tian et al., 2017) and DOAP (He et al., 2018). As done in (Balntas et al., 2016, Mishchuk et al., 2017, Tian et al., 2020, 2019), all the learning-based methods are trained on one subset, and then tested on the other two.

The false positive rates at 95% recall by all the comparative methods are reported in Table 1. As seen from this table, the performances of the three derived equal-weight student models are better than their corresponding teachers, and the derived DesDis-HyNet performs best among all

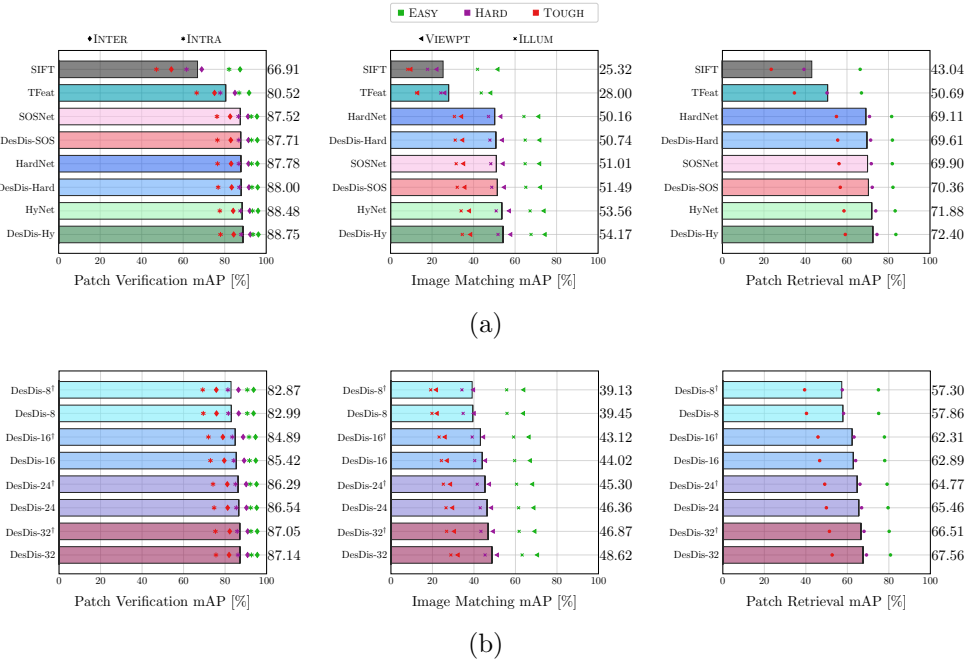


**Fig. 4** Comparison on the test set of split ‘a’ of the HPatches dataset (Balntas et al., 2020). (a) Evaluation on the derived equal-weight student models and several typical methods (Balntas et al., 2016, Lowe, 2004, Mishchuk et al., 2017, Tian et al., 2020, 2019). ‘DesDis-Hard’, ‘DesDis-SOS’ and ‘DesDis-Hy’ denote DesDis-HardNet, DesDis-SOSNet and DesDis-HyNet respectively. (b) Evaluation on the derived light-weight student models trained with/without the proposed teacher-student regularizer. ‘†’ denotes the baseline models that are trained without the proposed teacher-student regularizer.

the comparative methods. These results demonstrate that the proposed DesDis framework with the designed TS regularizer could effectively boost the performances of the existing networks.

#### 4.3.2 Evaluation on HPatches

We evaluate the three derived equal-weight student models in comparison to their teacher models HardNet (Mishchuk et al., 2017), SOSNet (Tian et al., 2019), HyNet (Tian et al., 2020), the relatively shallow network TFeat (Balntas et al., 2016) and the handcrafted descriptor SIFT (Lowe, 2004).

As done in previous works (He et al., 2018, Mishchuk et al., 2017, Tian et al., 2020, 2019), we train the models on the *Liberty* subset of Brown, and then evaluate on the test split ‘a’ of HPatches. The corresponding mean Average Precision (mAP) of each method are reported in Fig. 4a. As seen from this figure, the derived student models outperform their teachers respectively, and the derived DesDis-HyNet (DesDis-Hy) performs best among all the comparative methods, which are consistent with those on the Brown dataset as reported above.

#### 4.3.3 Evaluation on ETH

The comparative evaluation results on the ETH benchmark are reported above the dashed lines in Table 2. As seen from this table, SIFT obtains the smallest re-projection error, and a method that obtains a smaller number of matching points is prone to obtaining a lower re-projection error, which is consistent with the observations in (Luo et al., 2018, Tian et al., 2020, 2019). However, since the calculated re-projection errors by all the comparative methods are smaller than 1 pixel, this metric might not sufficiently reflect the performance differences among different descriptors as indicated in (Tian et al., 2019). It is further noted that the derived equal-weight student models achieve close performances to their teachers on the two small-scale high-quality sequences *Herzjesu* and *Fountain*. But for the two large-scale sequences (*Madrid Metropolis* and *Gendarmenmarkt*) with high noises, compared with their teachers, the derived equal-weight student models obtain close mean track lengths and achieve significantly better performances under the three protocols (the number of the registered images, the number of the reconstructed sparse points and

**Table 2** Evaluation results on the ETH benchmark (Schönberger et al., 2017) for SfM tasks. ‘†’ denotes the baseline models that are trained without the proposed teacher-student regularizer. The best results among equal-weight models are marked in red. The best results among our light-weight models are marked in blue.

		#Reg. Images	#Sparse Points	#Observations	Track Length	Reproj. Error
<b>Herzjesu 8 images</b>	SIFT	8	7.7K	30K	3.90	0.39px
	TFeat	8	7.7K	30K	3.90	0.41px
	HardNet	8	8.8K	36K	4.04	0.44px
	DesDis-HardNet	8	8.7K	36K	4.05	0.44px
	SOSNet	8	8.8K	36K	4.06	0.44px
	DesDis-SOSNet	8	8.8K	36K	4.06	0.44px
	HyNet	8	8.9K	36K	4.05	0.45px
	DesDis-HyNet	8	9.1K	37K	4.05	0.45px
	DesDis-8 <sup>†</sup>	8	8.4K	33.8K	4.03	0.42px
	DesDis-8	8	8.4K	34.0K	4.03	0.42px
	DesDis-32 <sup>†</sup>	8	8.6K	34.7K	4.04	0.45px
	DesDis-32	8	8.7K	35.2K	4.04	0.43px
<b>Fountain 11 images</b>	SIFT	11	16.6K	76K	4.57	0.34px
	TFeat	11	16.4K	75K	4.55	0.35px
	HardNet	11	17.7K	83K	4.69	0.38px
	DesDis-HardNet	11	17.7K	83K	4.69	0.38px
	SOSNet	11	17.7K	83K	4.71	0.38px
	DesDis-SOSNet	11	17.7K	84K	4.71	0.38px
	HyNet	11	17.9K	84K	4.70	0.39px
	DesDis-HyNet	11	18.0K	85K	4.71	0.39px
	DesDis-8 <sup>†</sup>	11	17.3K	81K	4.65	0.36px
	DesDis-8	11	17.4K	81K	4.66	0.37px
	DesDis-32 <sup>†</sup>	11	17.5K	82K	4.68	0.38px
	DesDis-32	11	17.7K	83K	4.67	0.38px
<b>Madrid Metropolis 1344 images</b>	SIFT	424	93K	562K	6.02	0.59px
	TFeat	402	81K	479K	5.89	0.61px
	HardNet	460	129K	778K	6.05	0.66px
	DesDis-HardNet	478	134K	799K	5.96	0.68px
	SOSNet	472	130K	793K	6.09	0.68px
	DesDis-SOSNet	481	137K	810K	5.93	0.67px
	HyNet	478	141K	840K	5.94	0.68px
	DesDis-HyNet	486	145K	847K	5.86	0.69px
	DesDis-8 <sup>†</sup>	436	107K	671K	6.25	0.64px
	DesDis-8	448	117K	704K	6.02	0.64px
	DesDis-32 <sup>†</sup>	449	125K	747K	5.96	0.66px
	DesDis-32	455	127K	769K	6.04	0.67px
<b>Gendar- menmarkt 1463 images</b>	SIFT	936	304K	1449K	4.76	0.72px
	TFeat	900	274K	1266K	4.61	0.75px
	HardNet	993	368K	1900K	5.16	0.78px
	DesDis-HardNet	994	373K	1919K	5.14	0.79px
	SOSNet	986	371K	1917K	5.17	0.78px
	DesDis-SOSNet	1021	401K	2042K	5.09	0.77px
	HyNet	982	386K	1993K	5.17	0.79px
	DesDis-HyNet	994	389K	2016K	5.17	0.79px
	DesDis-8 <sup>†</sup>	971	339K	1726K	5.10	0.76px
	DesDis-8	977	338K	1732K	5.12	0.76px
	DesDis-32 <sup>†</sup>	972	362K	1846K	5.10	0.77px
	DesDis-32	1017	400K	2019K	5.05	0.77px

**Table 3** Comparison of inference speeds (average number of images processed per second) on the HPatches dataset with 2048 keypoints. All the methods are evaluated on a GTX 1650Ti GPU with a batch size of 1024.

Method	Throughputs (images/sec)
TFeat	72
L2Nte	14
DOAP	14
HardNet/	14
DesDis-HardNet	14
SOSNet/	14
DesDis-SOSNet	14
HyNet/	9
DesDis-HyNet	9
DesDis-8	239
DesDis-16	210
DesDis-24	126
DesDis-32	99

the number of observations) in most cases, showing that the derived models under DesDis are more effective for handling large-scale noisy data.

#### 4.4 Light-Weight Student Models Under DesDis

In this subsection, we evaluate the efficiency of the proposed framework for deriving light-weight student models. As done in the above evaluation on the equal-weight models, the derived light-weight models are also evaluated on Brown, HPatches and ETH, in comparison to several state-of-the-arts methods. Moreover, we evaluate the architectures of these light-weight models trained with only the loss term from HyNet (Tian et al., 2020) as baselines for further demonstrating the effectiveness of the proposed TS regularizer, denoted as DesDis-8<sup>†</sup>, DesDis-16<sup>†</sup>, DesDis-24<sup>†</sup>, DesDis-32<sup>†</sup> respectively.

##### 4.4.1 Evaluation on Brown

The false positive rates at 95% recall by these light-weight models on the Brown dataset (Brown et al., 2010) are reported in Table 1. In addition, as done in (Balntas et al., 2016, Tian et al., 2017), the numbers of patches processed per second by the comparative methods are also reported in Table 1 for comparing their inference speeds. The following three points are observed from this table: (i) All the light-weight student models surpass their baselines that are trained without the

proposed TS regularizer, demonstrating the effectiveness of the designed TS regularizer for improving the performances of light-weight models; (ii) Compared with SOSNet (Tian et al., 2019) and HyNet (Tian et al., 2020), the light-weight student models achieve worse performances, but smaller computational memories and faster speeds. This is mainly because the light-weight student models need much fewer parameters and much simpler architectures as in Table 1, their ability of feature representation is weakened accordingly, but their computational costs are significantly decreased; (iii) Compared with TFeat (Balntas et al., 2016) which is a relatively fast descriptor in the existing works, our smallest student model DesDis-8 achieves a significantly better performance with a much faster speed. With slightly or significantly better performances, our light-weight models achieve 8 times or even faster speeds for processing patches (e.g. DesDis-16 vs L2Net:  $\approx 17.3$  times faster; DesDis-32 vs HardNet/DOAP:  $\approx 8.5$  times faster).

##### 4.4.2 Evaluation on HPatches

The comparative results of the light-weight models with/without the TS regularizer on the HPatches dataset (Balntas et al., 2020) are reported in Fig. 4b. As seen from this figure, the derived models (DesDis-8, DesDis-16, DesDis-24, DesDis-32) with the TS regularizer consistently outperform their counterparts without it. These results further demonstrate the effectiveness of the designed TS regularizer. In addition, in order to further compare the inference speeds of the comparative methods for images (rather than patches as reported in Table 1), Table 3 reports the average number of images processed per second on the HPatches benchmark, including 6 existing methods (TFeat, L2Net, DOAP, HardNet, SOSNet, HyNet), the proposed 3 equal-weight student models (DesDis-HardNet, DesDis-SOSNet, DesDis-HyNet), and the proposed 4 light-weight student models (DesDis-8, DesDis-16, DesDis-24, DesDis-32). All the methods use a fixed number (2048) of keypoints, and are evaluated on a 1650Ti GPU with a batch size of 1024. As seen from this table, our light-weight student models still have significantly faster inference speeds than the other comparative methods.

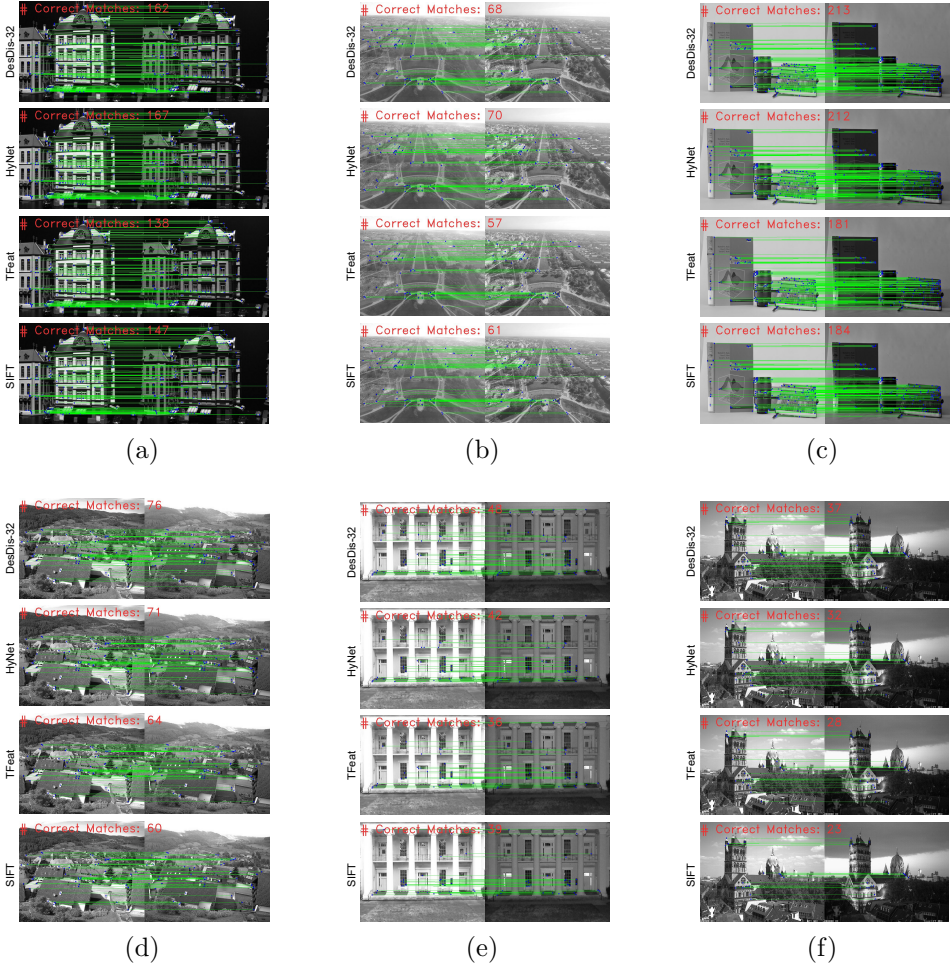


**Fig. 5** Image matching visualization on HPatches by the proposed DesDis-32, HyNet, TFeat and SIFT. The models are trained on the Liberty subset of Brown. The number of correct matches is shown in the upper left corner of each image pair.

#### 4.4.3 Evaluation on ETH

Considering that it is much time-consuming to perform the structure from motion task on large-scale scenes in the ETH dataset (Schönberger et al., 2017), we only evaluate the smallest variant DesDis-8 and the largest variant DesDis-32 among the derived four light-weight models, as well as their baseline models DesDis-8<sup>†</sup> and DesDis-32<sup>†</sup> respectively. The results are reported in Table 2. As noted from this table, in terms of the numbers of registered images, reconstructed sparse points and observations, DesDis-8 and DesDis-32 perform better than SIFT (Lowe, 2004), TFeat (Balntas et al., 2016) and their corresponding baselines. It's also worth noting that in terms of the aforementioned 3 metrics, our DesDis-32 can surpass HardNet, SOSNet and HyNet on the

largest scene *Gendarmenmarkt*, and it achieves a close performance to HardNet on other scenes with an 8.5 times faster speed. All the results demonstrate that the derived light-weight models from the proposed DesDis framework could achieve an effective trade-off between computational accuracy and speed.

#### 4.4.4 Visualization Results

We provide several image matching visualization results from the HPatches dataset (Balntas et al., 2020) by the proposed light-weight model DesDis-32 and three typical descriptors, including the DesDis-32's teacher model HyNet (Tian et al., 2020), TFeat (Balntas et al., 2016) (a relatively fast descriptor in literature) and the hand-crafted SIFT (Lowe, 2004). The keypoints are all detected

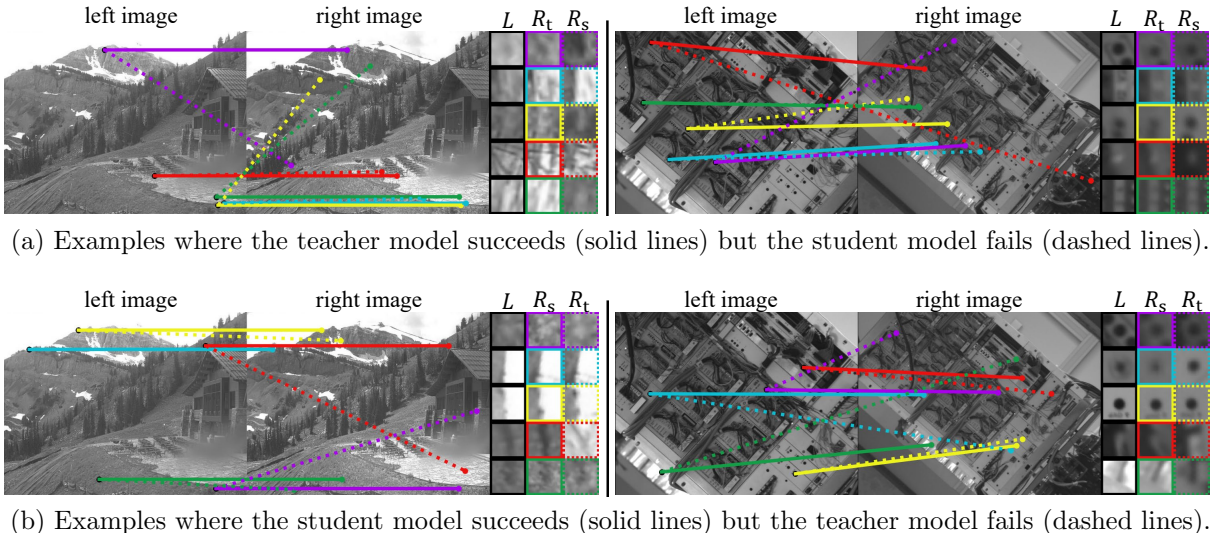


**Fig. 6** Visualization of the keypoint matches by the teacher HyNet and the corresponding student DesDis-32 on HPatches. The left part of each group shows a pair of images, where five point matches by both the teacher and student are connected with colorful lines. The right part of each group shows the corresponding local patches to the five keypoints, and in each row,  $L$  corresponds to a keypoint in the left image,  $R_t$  corresponds to the matched keypoint by the teacher in the right image, and  $R_s$  corresponds to the matched keypoint by the student in the right image.

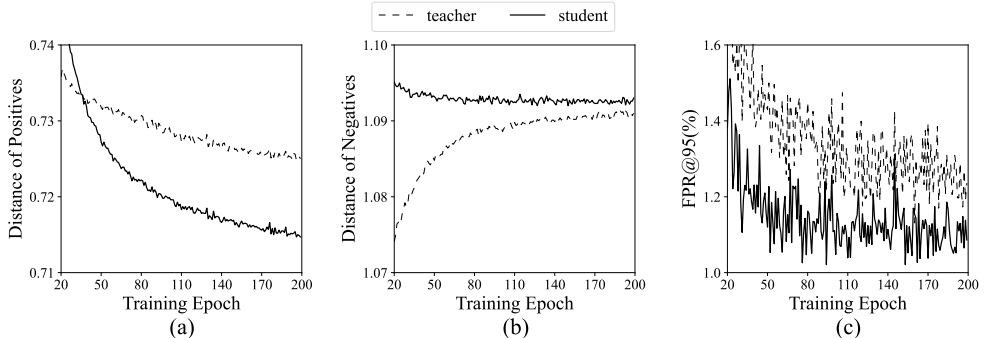


**Fig. 7** Comparison of positive/negative pair distance and the model performance during training. The model is trained on the Liberty subset of the Brown dataset, and then tested on the Yosemite and Notredame subsets. (a) The distance of positive pairs during the training procedure. (b) The distance of negative pairs during the training procedure. (c) The false positive rate at 95% recall during training.

by the DoG detector. As seen from Fig. 5a-5f, DesDis-32 and HyNet are able to obtain a larger number of correct correspondences than SIFT and TFeat. In most cases, DesDis-32 could achieve a close number of correct matches to HyNet (Fig. 5a-5c), while in some challenging scenes, DesDis-32 could even produce more correct matches (Fig. 5d-5f). It has to be pointed out that the complex architecture of HyNet results in a small throughput (12K patch/sec on a GTX 1650Ti), and our light-weight model DesDis-32 runs at 145K patch/sec (12 $\times$  faster) while maintaining a comparable image matching accuracy.

Fig. 6 further compares the keypoint matching results by the teacher HyNet and its student DesDis-32 respectively (including wrongly/correctly matched keypoint and their corresponding local patches) on HPatches. Fig. 6a shows the cases that succeed in the teacher model but fail in the student model. Fig. 6b shows the cases that succeed in the student model but fail in the teacher model. It is found from these two figures that local patches with similar textures are challenging for both the teacher and student models, in other words, for a same pair of images, the teacher succeeds in discriminating some pairs of local patches with similar textures whereas the

student fails, and the teacher also fails in discriminating some other pairs of local patches with similar textures whereas the student succeeds.

## 4.5 Ablation Study

### 4.5.1 Impact of the Proposed TS Regularizer

As analyzed in Section 3.4, the TS regularizer could help the student model predict a smaller distance of positive pairs and a larger distance for negative pairs than its teacher network, leading to a better performance. To verify this theoretical analysis, we firstly record the mean distance of positive pairs (also negative pairs) by the teacher and student models on the *Liberty* subset of the Brown dataset (Brown et al., 2010) at each training epoch. Accordingly, we visualize the corresponding curves of the mean distance of positive pairs in Fig. 7a, as well as the curves of the mean distance of negative pairs in Fig. 7b. As seen from the two figures, when the number of epochs becomes larger than around 40, the student could predict a smaller distance for positive pairs than its teacher, and a larger distance for negative pairs. These results demonstrate the aforementioned deduction from Proposition 1 to some extent. Secondly, for each trained model corresponding to each training epoch on the *Liberty* subset, we test it on the other two subsets of the Brown dataset and record its mean false positive rate at 95% recall. Accordingly, we visualize the corresponding false positive rate curves of the teacher and student models in Fig. 7c. As seen from this figure, the student model could outperform its teacher. It is also noted that the distance differences between the student and teacher model illustrated in Fig. 7a and Fig. 7b is smaller than the optimal solution indicated by Eqn. (7), indicating the student model could not find the global optimal solution. However, it should be pointed out that Proposition 1 is not intended to prove whether a student model could obtain a globally optimal solution or not, but to provide a theoretical basis (regardless of whether a globally optimal solution could be obtained or not) that the distances of positive pairs in the student model would become smaller than those in the teacher model at the training stage, while the distances of negative pairs in the student model would become larger than those in the teacher model.

**Table 4** Results by setting the distance supervision  $d_p$  for positive pairs to  $\{0.5, 0.6, 0.7\}$  and the distance supervision  $d_n$  for negative pairs to  $\{1.0, 1.1, 1.2\}$ . The numbers in the three columns on the right are the false positive rate at 95% recall.

Method	YOS $\downarrow$	ND $\downarrow$	Mean $\downarrow$
HyNet (baseline)	0.88	0.34	0.61
$d_p = 0.5, d_n = 1.0$	1.40	0.35	0.88
$d_p = 0.5, d_n = 1.1$	1.18	0.35	0.76
$d_p = 0.5, d_n = 1.2$	1.11	0.31	0.71
$d_p = 0.6, d_n = 1.0$	1.10	0.36	0.73
$d_p = 0.6, d_n = 1.1$	1.22	0.32	0.77
$d_p = 0.6, d_n = 1.2$	0.92	0.34	0.63
$d_p = 0.7, d_n = 1.0$	1.05	0.35	0.70
$d_p = 0.7, d_n = 1.1$	0.94	0.39	0.67
$d_p = 0.7, d_n = 1.2$	0.99	0.37	0.68
<b>DesDis-HyNet</b>	<b>0.70</b>	<b>0.29</b>	<b>0.50</b>

To further evaluate the importance of the proposed TS regularizer, we conduct the following experiment by replacing the teacher supervisions in the TS regularizer with fixed distance supervisions, i.e., we replace the positive distances predicted by the teacher model in Eqn. (1) with a fixed low distance  $d_p$ , and replace the negative distances in Eqn. (2) with a fixed high distance  $d_n$ : Firstly, we train HyNet (Tian et al., 2020) on the *Liberty* subset of Brown, and obtain the mean distance of descriptor pairs (around 0.7 for positive pairs and 1.0 for negative pairs) on the *Liberty* subset by HyNet. Then, considering that the mean distance of positive/negative pairs of HyNet is approximately 0.7/1.0, we train DesDis-HyNet by setting  $d_p$  for positive pairs to  $\{0.5, 0.6, 0.7\}$ , and  $d_n$  for negative pairs to  $\{1.0, 1.1, 1.2\}$ . The corresponding results are shown in Table 4. As seen from this table, such fixed distances does not work as well as using a teacher model under the proposed framework. It could be further noted that the results (particularly on the *Yosemite* subset) by fixed distance supervisions are even poorer than those by the baseline HyNet in most cases, indicating that fixed distance supervisions might not be helpful for improving model performances.

### 4.5.2 Impact of $\alpha_p$ and $\alpha_n$

In this subsection, we evaluate the effect of the two weights  $\alpha_p$  and  $\alpha_n$  in Eqn. (3). It is noted from many visual tasks: when a set of training data is used to respectively train two networks that

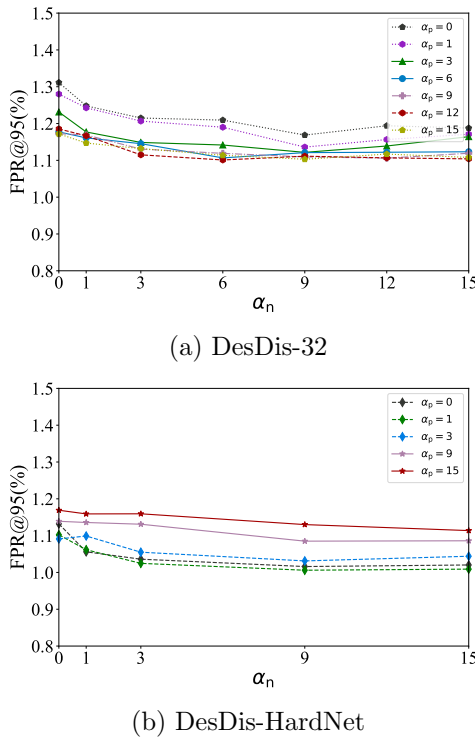


**Fig. 8** Impact of  $\alpha_p$  and  $\alpha_n$  on the light-weight student (a) DesDis-32, and the equal-weight student (b) DesDis-HardNet. The models are trained on the Liberty subset of the Brown dataset, and then evaluated on the Yosemite and Notre Dame subsets. The results under each parameter configuration are averaged over 5 reruns.

have a completely same loss function (often containing multiple weighted loss terms) but different architectures (e.g., different numbers of layers), their performances would be generally different. An appropriate weight configuration of loss terms for one network might not be quite appropriate for the other. Hence, we conduct experiments on light-weight and equal-weight student models respectively. In the light-weight student case, we evaluate DesDis-32 under different configurations of  $\alpha_p = \{0, 1, 3, 6, 9, 12, 15\}$  and  $\alpha_n = \{0, 1, 3, 6, 9, 12, 15\}$ . We train the model on the *Liberty* subset of Brown, and then test it on the *Yosemite* and *Notredame* subsets. We evaluate the model under each parameter configuration five times independently. The corresponding mean results are shown in Fig. 8a. As seen from this table, when the two weights vary from 6 to 15, the performance of DesDis-32 varies slowly, indicating that the proposed TS regularizer is not quite sensitive to the two weights. So the two parameters

**Table 5** Impact of  $\mathcal{L}_B$ . The models are trained on the *Liberty* subset of Brown, and tested on the *Yosemite* (YOS) and *Notredame* (ND) subsets. The numbers are false positive rate at 95% recall.

Method	YOS↓	ND↓	Mean↓
HyNet	0.88	0.34	0.61
DesDis-HyNet (w/o $\mathcal{L}_B$ )	0.93	0.35	0.64
DesDis-HyNet (with $\mathcal{L}_B$ )	<b>0.70</b>	<b>0.29</b>	<b>0.50</b>

are simply set to 9 for the proposed light-weight models in all the experiments. In the equal-weight student case, we evaluate DesDis-HardNet under different configurations of  $\alpha_p = \{0, 1, 3, 9, 15\}$  and  $\alpha_n = \{0, 1, 3, 9, 15\}$ . We train the model on the *Liberty* subset of Brown, and then test it on the *Yosemite* and *Notredame* subsets. We evaluate the model under each parameter configuration five times independently. The corresponding mean results are shown in Fig. 8b. As seen from this figure, when  $\alpha_p = 1$  and  $\alpha_n$  varies from 9 to 15, the model varies slightly and performs better in comparison to the other parameter configurations. So,  $\alpha_p$  is set to 1 and  $\alpha_n$  is set to 15 for the equal-weight models in all the experiments.

#### 4.5.3 Impact of $\mathcal{L}_B$

In this subsection, we evaluate the impact of the basic loss term  $\mathcal{L}_B$  in Eqn. (3). Here, we use HyNet (Tian et al., 2020) as the teacher model, and derive the corresponding equal-weight student model that is trained only with the TS regularizer (without  $\mathcal{L}_B$ ) in Eqn. (3). The *Liberty* subset of the Brown dataset is used for training, and the *Yosemite* and *Notredame* subsets are used for testing. The corresponding results are reported in Table 5. In addition, the corresponding results by the original HyNet (baseline) and our complete model DesDis-HyNet with  $\mathcal{L}_B$  are also added into Table 5 for comparison. As seen from this table, the performance of the model trained without  $\mathcal{L}_B$  is slightly worse than that of the original HyNet, and also worse than that of the proposed complete model trained with both  $\mathcal{L}_B$  and the TS regularizer. These results demonstrate that the joint usage of both  $\mathcal{L}_B$  and the proposed TS regularizer is much helpful for improving performances.

**Table 6** Comparison among the light-weight student models with  $\{3, 4, 5, 6\}$  layers (denoted as Net-I, Net-II, Net-III, Net-IV, and Net-III is exactly DesDis-32). The numbers in the seven columns on the right are the false positive rates at 95% recall on Brown (Brown et al., 2010). The throughputs are tested on a GTX 1650Ti.

Train	#Layers	#Param.	Throughputs	ND	YOS	LIB	YOS	LIB	ND	Mean
Test			(K patch/sec)	LIB		ND		YOS		
Net-I	3	0.543M	261	3.87	4.78	1.09	1.57	3.83	3.04	3.03
Net-II	4	0.355M	195	2.07	2.95	0.61	0.94	2.16	2.10	1.81
<b>Net-III</b>	5	0.502M	145	1.52	2.36	0.54	<b>0.81</b>	<b>1.68</b>	1.48	1.39
Net-IV	6	0.539M	102	<b>1.35</b>	<b>2.11</b>	<b>0.46</b>	0.82	1.76	<b>1.33</b>	<b>1.31</b>

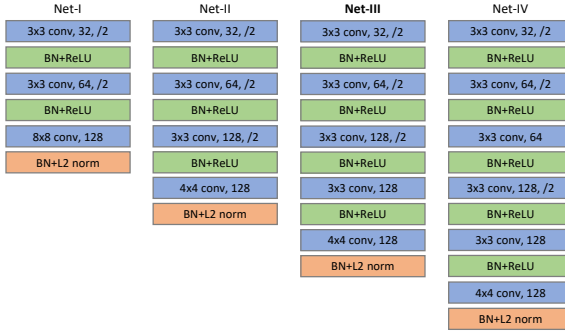


**Fig. 9** Architectures of the four models with  $\{3, 4, 5, 6\}$  convolutional layers. ‘BN’ denotes batch normalization. ‘/2’ denotes convolution operation with a stride of 2. Net-III is exactly the DesDis-32 in Section 4.

#### 4.5.4 Impact of the Number of Layers in the Light-Weight Models

Considering that we have tested four 5-layer student models with different numbers of channels in Section 4.4, we evaluate the performances of the student models with different numbers of layers in this subsection. Similar to the experimental configuration in Section 4.4, we adopt HyNet (Tian et al., 2020) as the teacher model. Then, we use the Brown dataset to evaluate four light-weight student models with  $\{3, 4, 5, 6\}$  layers respectively. The four models are denoted as Net-I, Net-II, Net-III, Net-IV, and Net-III is exactly the DesDis-32 in previous sections.

Fig. 9 shows the architectures of the four light-weight models. As seen from this figure, except the last convolutional layer that encodes the feature maps into a 128 dimensional descriptor, all the rest convolutional layers in the four models have a kernel size of  $3 \times 3$ . The channel number in the first layer is 32, and is doubled whenever the feature map is downsampled through strided convolution. The third and fourth columns in Table 6 report the parameter numbers and the throughputs of the

four models. It is noted that among these models, although Net-I has only 3 layers, it has the largest number of parameters, mainly because it uses a large convolution kernel  $8 \times 8$  in its last layer. In addition, although Net-I has the largest number of parameters, its computational cost is the lowest, hence, it has the largest throughput. In general, with the increase of the layer number, a student model achieves a relatively smaller throughput.

Table 6 also reports the false positive rates at 95% recall by the four student models. As noted from this table, with the increase of the layer number, a student model generally achieves a relatively higher patch verification performance, but a relatively slower inference speed. Among them, Net-III could achieve a relatively better balance between computational efficiency and accuracy ( $\approx 1.4 \times$  faster than Net-IV without a significant drop in performance). Thus, we adopt 5-layer-networks in Section 4.

#### 4.6 Evaluation of DesDis by Utilizing Handcrafted Descriptor as Teacher

In the previous subsections, we have verified the effectiveness of the proposed DesDis framework for distilling the knowledge of DNN-based local descriptors. In this subsection, we further evaluate the effectiveness of DesDis for distilling the knowledge of the handcrafted descriptor, including SIFT (Lowe, 2004) and ORB (Rublee et al., 2011).

##### 4.6.1 SIFT Distillation Under DesDis

Here, we use the classic SIFT (Lowe, 2004) as the teacher and DesDis-32 as the student. We compare the following variants on the Brown dataset (Brown et al., 2010): (1) the model trained with only the proposed TS regularizer, denoted as Model #1; (2) the model trained with both the

**Table 7** Evaluation on the loss terms of the DesDis framework by utilizing the handcrafted descriptor as teacher.  $\mathcal{L}_B$  denotes the basic loss term from HyNet. TSR denotes the teacher-student regularizer. The numbers denote the false positive rate at 95% recall.

Train	$\mathcal{L}_B$	TSR	ND	YOS	LIB	YOS	LIB	ND	Mean
			LIB	ND	LIB	YOS	LIB	ND	
Test									
SIFT			29.86		22.53		27.29		26.55
#1 DesDis-32 (SIFT as teacher)		✓	32.03	31.05	19.71	20.21	25.34	25.55	25.65
#2 DesDis-32 (SIFT as teacher)	✓	✓	1.83	2.78	0.51	0.95	2.15	1.71	1.67
#3 DesDis-32 (without distillation)	✓		1.81	2.86	0.55	0.90	2.01	1.69	1.64
DesDis-32 (HyNet as teacher)	✓	✓	1.52	2.36	0.54	0.81	1.68	1.48	1.39
ORB			57.37		49.05		53.65		53.36
Binary DesDis-32 (ORB as teacher) V1		✓	60.81	65.17	45.24	49.83	58.24	57.12	56.06
Binary DesDis-32 (ORB as teacher) V2		✓	58.61	58.09	48.34	45.84	53.85	52.16	52.82

TS regularizer and the basic loss term  $\mathcal{L}_B$  from HyNet, denoted as Model #2; (3) the DesDis-32 that is singly trained with  $\mathcal{L}_B$  (without distillation), denoted as Model #3.

The corresponding results are reported at the top of Table 7. In addition, Table 7 also reports the results of SIFT and the proposed DesDis-32 by utilizing HyNet (Tian et al., 2020) as teacher for comparison. The following points could be observed from this table:

(1) Model #1 that is trained with only the TS regularizer by utilizing SIFT as teacher could achieve a slightly better performance than SIFT. This verifies the transferability of handcrafted descriptor into an end-to-end network to some extent, however, the improvement brought by the end-to-end network with the TS regularizer is limited.

(2) Model #2 that is trained with both the basic loss term  $\mathcal{L}_B$  and the TS regularizer by utilizing SIFT as the teacher model significantly outperforms SIFT and Model #1. However, it is noted from Table 7 that Model #2 only achieves a close performance to Model #3, which is singly trained with  $\mathcal{L}_B$  but does not use SIFT for distillation. These results indicate that when the handcrafted descriptor SIFT is used as teacher, the improvement of its student mainly owes to the basic loss  $\mathcal{L}_B$ , rather than the teacher SIFT and the TS regularizer, probably because the performance of the teacher SIFT is significantly worse than the singly trained Model #3.

(3) The proposed DesDis-32 with both  $\mathcal{L}_B$  and the TS regularizer by utilizing HyNet as the teacher model performs best among all the comparative methods. This result indicates that when

a relatively high-quality model (e.g., HyNet) is used as teacher, its student would obtain more benefits from the designed TS regularizer.

#### 4.6.2 ORB Distillation Under DesDis

In the previous content, we focused on learning and distilling the knowledge of real-valued descriptors. In this subsection, we analyze the possibility of knowledge distillation of binary descriptors in the proposed DesDis framework. Here, we use the classic ORB (Rublee et al., 2011) descriptor as teacher.

For knowledge distillation of ORB in DesDis, the following issues have to be taken into account: (i) the designed Teacher-Student (TS) regularizer in DesDis has to measure the difference between the distance of pairwise binary teacher descriptors (i.e., ORB) and the distance of pairwise student descriptors, however, the commonly-used distance metric for ORB is the Hamming distance, different from the Euclidean distance metric used for the real-valued student descriptors in the current version of DesDis; (ii) it is generally more difficult for a deep network to learn a binary descriptor than a real-valued descriptor in an end-to-end manner from the perspective of network training optimization.

It is noted that many existing binary descriptor learning methods (He et al., 2018, Tian et al., 2017) employ a two-stage strategy: they firstly train a deep network for learning real-valued descriptors, and then binarize the real-valued descriptors as a post-processing operation. Considering that such a two-stage strategy could avoid the aforementioned second issue, we attempt to use this strategy for knowledge distillation of ORB

**Table 8** Comparison of training time (second) on the *Liberty* subset of Brown. The models are trained for 200 epochs on a Tesla V100 GPU. The forward propagation when training a teacher only involves the forward propagation of itself, while the forward propagation when training a student involves the forward propagation of itself and its teacher.

Model	Forward Propagation	Loss Computation	Backward Propagation	Total
HardNet	1208	125	3051	4384
DesDis-HardNet	2118	262	3052	5432
SOSNet	1210	283	3030	4523
DesDis-SOSNet	2118	408	3042	5568
HyNet	1411	153	4864	6428
DesDis-HyNet	2453	284	4865	7602

here. Accordingly, in order to handle the aforementioned first issue, we use the following two variants of the TS regularizer respectively for network training: (V1) we scale the Hamming distance of pairwise teacher ORB descriptors into the range [0, 2] where the Euclidean distances of pairwise normalized student descriptors vary, and then measure the difference between the student and teacher distances; (V2) we calculate the Euclidean distances (also scaled into the range [0, 2]) of pairwise ORB descriptors instead of the Hamming distance, and then measure the difference between the student and teacher distances. The corresponding results on the Brown dataset (Brown et al., 2010) by utilizing DesDis-32 as the student model are reported in Table 7 above. As seen from this table, DesDis-32 that is trained with the V1 variant performs slightly worse than ORB, while DesDis-32 that is trained with the V2 variant performs slightly better than ORB. These results demonstrate the possibility of knowledge distillation of binary descriptors to some extent.

#### 4.7 Comparison of Training Time of the Teacher and Student

In this subsection, we evaluate the training time costs of the teacher and student models. Specifically, we compare the training times of the three teacher models HardNet (Mishchuk et al., 2017), SOSNet (Tian et al., 2019) and HyNet (Tian et al., 2020), with their corresponding student models DesDis-HardNet, DesDis-SOSNet and DesDis-HyNet respectively. All the models are trained on the *Liberty* subset of the Brown dataset for 200 epochs on a Tesla V100 GPU. The corresponding training time costs of these models are reported in Table 8.

As seen from the table, the time cost for training a model consists of three parts: the forward propagation time, the loss computation time, and the back propagation time. And three points could be observed:

(1) Each proposed distillation method takes nearly twice forward propagation times as long as its corresponding baseline method, because the forward propagations of both the student and teacher models have to be implemented when training the proposed distillation method.

(2) The loss computation time of each proposed method is larger than that of its corresponding baseline method, because the additional TS regularizer has to be computed in the proposed method. However, the training times of both the proposed method and its baseline for loss computation are much smaller than those for forward and backward propagations.

(3) The training times of each proposed method and its baseline for back propagation are close, because the student model in the proposed equal-weight method (where the teacher model is always frozen) has the same architecture as its baseline. Additionally, the back propagation times of each proposed method and its baseline are much larger than their forward propagation times, mainly because of the gradient computations involved during the back propagation process.

In sum, training an equal-weight student model takes around 1.2 times as long as training a teacher model.

## 5 Conclusion

In this paper, we focus on learning a fast and discriminative local descriptor. Many existing works

in literature employed a triplet loss or its variants that are expected to enforce a small distance between positive pairs and a large distance between negative pairs. However, such an expectation has to be lowered due to the non-perfect convergence of the networks. Addressing this issue, we propose a descriptor distillation framework, named DesDis, for local descriptor learning, where a student model gains knowledge from its teacher. In addition, we prove in theory that the student model could outperform its teacher through the designed teacher-student regularizer. Under the proposed DesDis framework, both equal-weight and light-weight student models could be obtained. Extensive experimental results on 3 public datasets demonstrate that the proposed DesDis framework could not only boost the performances of the existing descriptor learning networks by utilizing them as the teacher models, but also pursue much lighter student models that achieve a balance between computational effectiveness and efficiency.

**Acknowledgment** This work is funded by the National Natural Science Foundation of China (Grant Nos. 61991423, 62376269) and the Strategic Priority Research Program of the Chinese Academy of Sciences (Grant No. XDA27040811).

**Data Availability Statement** The public datasets used in this paper are: (a) the Brown dataset (Brown et al., 2010), (b) the HPatches dataset (Balntas et al., 2020), and (c) the ETH SfM dataset (Schönberger et al., 2017). (a) is available at <http://matthewalunbrown.com/patchdata/patchdata.html>, (b) is available at <https://github.com/hpatches/hpatches-dataset>, and (c) is available at <http://www.cvg.ethz.ch/research/local-feature-evaluation/>

## References

Balntas, V., Lenc, K., Vedaldi, A., Tuytelaars, T., Matas, J., and Mikolajczyk, K. (2020). Hpatches: A benchmark and evaluation of hand-crafted and learned local descriptors. *IEEE Transactions on Pattern Analysis and Machine Intelligence*, 42(11).

Balntas, V., Riba, E., Ponsa, D., and Mikolajczyk, K. (2016). Learning local feature descriptors with triplets and shallow convolutional neural

networks. In *British Machine Vision Conference*, volume 1, page 3.

Bay, H., Ess, A., Tuytelaars, T., and Van Gool, L. (2008). Speeded-up robust features (surf). *Computer Vision and Image Understanding*, 110(3):346–359.

Bökman, G. and Kahl, F. (2022). A case for using rotation invariant features in state of the art feature matchers. In *Proceedings of the IEEE/CVF Conference on Computer Vision and Pattern Recognition*, pages 5110–5119.

Brown, M., Hua, G., and Winder, S. (2010). Discriminative learning of local image descriptors. *IEEE Transactions on Pattern Analysis and Machine Intelligence*, 33(1):43–57.

Brown, M. and Lowe, D. G. (2007). Automatic Panoramic Image Stitching using Invariant Features. *International Journal of Computer Vision*, pages 59–73.

Dong, J. and Soatto, S. (2015). Domain-size pooling in local descriptors: Dsp-sift.

Dong, Q., Gao, X., Cui, H., and hu, Z. (2020). Robust camera translation estimation via rank enforcement. *IEEE Transactions on Cybernetics*, 52(2):862–872.

Dusmanu, M., Miksik, O., Schönberger, J. L., and Pollefeys, M. (2021). Cross-descriptor visual localization and mapping. In *Proceedings of the IEEE International Conference on Computer Vision*, pages 6058–6067.

Dusmanu, M., Rocco, I., Pajdla, T., Pollefeys, M., Sivic, J., Torii, A., and Sattler, T. (2019). D2-Net: A Trainable CNN for Joint Detection and Description of Local Features. In *Proceedings of the IEEE/CVF Conference on Computer Vision and Pattern Recognition*, pages 8092–8101.

Faghri, F., Fleet, D. J., Kiros, J. R., and Fidler, S. (2018). Vse++: Improving visual-semantic embeddings with hard negatives.

Han, X., Leung, T., Jia, Y., Sukthankar, R., and Berg, A. C. (2015). Matchnet: Unifying feature

and metric learning for patch-based matching. In *Proceedings of the IEEE/CVF Conference on Computer Vision and Pattern Recognition*, pages 3279–3286.

He, K., Lu, Y., and Sclaroff, S. (2018). Local descriptors optimized for average precision. In *Proceedings of the IEEE/CVF Conference on Computer Vision and Pattern Recognition*, pages 596–605.

He, T., Shen, C., Tian, Z., Gong, D., Sun, C., and Yan, Y. (2019). Knowledge adaptation for efficient semantic segmentation. In *Proceedings of the IEEE/CVF Conference on Computer Vision and Pattern Recognition*, pages 578–587.

Herrmann, C., Wang, C., Bowen, R. S., Keyder, E., Krainin, M., Liu, C., and Zabih, R. (2018). Robust image stitching with multiple registrations. In *European Conference on Computer Vision*, pages 53–67.

Hinton, G., Vinyals, O., Dean, J., et al. (2015). Distilling the knowledge in a neural network. *arXiv preprint arXiv:1503.02531*, 2.

Hou, Y., Ma, Z., Liu, C., Hui, T.-W., and Loy, C. C. (2020). Inter-region affinity distillation for road marking segmentation. In *Proceedings of the IEEE/CVF Conference on Computer Vision and Pattern Recognition*, pages 12486–12495.

Huang, Y., Wu, J., Xu, X., and Ding, S. (2022). Evaluation-oriented knowledge distillation for deep face recognition. In *Proceedings of the IEEE/CVF Conference on Computer Vision and Pattern Recognition*, pages 18740–18749.

Huang, Z., Zou, Y., Bhagavatula, V., and Huang, D. (2020). Comprehensive attention self-distillation for weakly-supervised object detection. In *Neural Information Processing Systems*, volume 33, pages 16797–16807.

Ke, Y. and Sukthankar, R. (2004). Pca-sift: a more distinctive representation for local image descriptors. In *Proceedings of the IEEE/CVF Conference on Computer Vision and Pattern Recognition*, volume 2.

Lee, J., Jeong, Y., Kim, S., Min, J., and Cho, M. (2021). Learning to distill convolutional features into compact local descriptors. In *Proceedings of the IEEE Winter Conference on Applications of Computer Vision*, pages 898–908.

Low, C.-Y., Teoh, A. B.-J., and Park, J. (2021). Mind-net: A deep mutual information distillation network for realistic low-resolution face recognition. *Signal Processing Letters*, 28:354–358.

Lowe, D. G. (2004). Distinctive image features from scale-invariant keypoints. *International Journal of Computer Vision*, 60(2):91–110.

Luo, P., Zhu, Z., Liu, Z., Wang, X., and Tang, X. (2016). Face model compression by distilling knowledge from neurons. In *Proceedings of the AAAI Conference on Artificial Intelligence*.

Luo, Z., Shen, T., Zhou, L., Zhu, S., Zhang, R., Yao, Y., Fang, T., and Quan, L. (2018). Geodesc: Learning local descriptors by integrating geometry constraints. In *European Conference on Computer Vision*, pages 168–183.

Luo, Z., Zhou, L., Bai, X., Chen, H., Zhang, J., Yao, Y., Li, S., Fang, T., and Quan, L. (2020). Aslfeat: Learning local features of accurate shape and localization. In *Proceedings of the IEEE/CVF Conference on Computer Vision and Pattern Recognition*, pages 6589–6598.

Ma, J., Jiang, X., Fan, A., Jiang, J., and Yan, J. (2021). Image matching from handcrafted to deep features: A survey. *International Journal of Computer Vision*, 129(1):23–79.

Ma, Z., Luo, G., Gao, J., Li, L., Chen, Y., Wang, S., Zhang, C., and Hu, W. (2022). Open-vocabulary one-stage detection with hierarchical visual-language knowledge distillation. In *Proceedings of the IEEE/CVF Conference on Computer Vision and Pattern Recognition*, pages 14074–14083.

Mishchuk, A., Mishkin, D., Radenovic, F., and Matas, J. (2017). Working hard to know your neighbor’s margins: Local descriptor learning loss. In *Neural Information Processing Systems*,

volume 30.

Ng, T., Balntas, V., Tian, Y., and Mikolajczyk, K. (2020). Solar: second-order loss and attention for image retrieval. In *European Conference on Computer Vision*, pages 253–270.

Nie, X., Li, Y., Luo, L., Zhang, N., and Feng, J. (2019). Dynamic kernel distillation for efficient pose estimation in videos. In *Proceedings of the IEEE/CVF Conference on Computer Vision and Pattern Recognition*, pages 6942–6950.

Noh, H., de Araújo, A. F., Sim, J., Weyand, T., and Han, B. (2017). Large-scale image retrieval with attentive deep local features. In *Proceedings of the IEEE International Conference on Computer Vision*, pages 3476–3485.

Pautrat, R., Larsson, V., Oswald, M. R., and Pollefeys, M. (2020). Online invariance selection for local feature descriptors. In *European Conference on Computer Vision*, pages 707–724.

Radenovic, F., Schönberger, J. L., Ji, D., Frahm, J.-M., Chum, O., and Matas, J. (2016). From dusk till dawn: Modeling in the dark. In *Proceedings of the IEEE/CVF Conference on Computer Vision and Pattern Recognition*, pages 5488–5496.

Revaud, J., De Souza, C., Humenberger, M., and Weinzaepfel, P. (2019). R2d2: Reliable and repeatable detector and descriptor. In *Neural Information Processing Systems*, volume 32.

Rublee, E., Rabaud, V., Konolige, K., and Bradski, G. (2011). Orb: An efficient alternative to sift or surf. In *2011 International conference on computer vision*, pages 2564–2571. Ieee.

Schonberger, J. L. and Frahm, J.-M. (2016). Structure-from-motion revisited. In *Proceedings of the IEEE/CVF Conference on Computer Vision and Pattern Recognition*, pages 4104–4113.

Schönberger, J. L., Zheng, E., Frahm, J.-M., and Pollefeys, M. (2016). Pixelwise view selection for unstructured multi-view stereo. In *European Conference on Computer Vision*, pages 501–518. Springer.

Schönberger, J. L., Hardmeier, H., Sattler, T., and Pollefeys, M. (2017). Comparative evaluation of hand-crafted and learned local features. In *Proceedings of the IEEE/CVF Conference on Computer Vision and Pattern Recognition*, pages 1482–1491.

Simo-Serra, E., Trulls, E., Ferraz, L., Kokkinos, I., Fua, P., and Moreno-Noguer, F. (2015). Discriminative learning of deep convolutional feature point descriptors. In *Proceedings of the IEEE International Conference on Computer Vision*, pages 118–126.

Sun, J., Shen, Z., Wang, Y., Bao, H., and Zhou, X. (2021). Loftr: Detector-free local feature matching with transformers. In *Proceedings of the IEEE/CVF Conference on Computer Vision and Pattern Recognition*, pages 8922–8931.

Tian, Y., Barroso-Laguna, A., Ng, T., Balntas, V., and Mikolajczyk, K. (2020). Hynet: Learning local descriptor with hybrid similarity measure and triplet loss. In *Neural Information Processing Systems*, volume 33, pages 7401–7412.

Tian, Y., Fan, B., and Wu, F. (2017). L2-net: Deep learning of discriminative patch descriptor in euclidean space. In *Proceedings of the IEEE/CVF Conference on Computer Vision and Pattern Recognition*, pages 661–669.

Tian, Y., Yu, X., Fan, B., Wu, F., Heijnen, H., and Balntas, V. (2019). Sosnet: Second order similarity regularization for local descriptor learning. In *Proceedings of the IEEE/CVF Conference on Computer Vision and Pattern Recognition*, pages 11016–11025.

Tyszkiewicz, M., Fua, P., and Trulls, E. (2020). Disk: Learning local features with policy gradient. *Neural Information Processing Systems*, 33:14254–14265.

Wang, C., Zhang, X., and Lan, X. (2017). How to train triplet networks with 100k identities? In *Proceedings of the IEEE International Conference on Computer Vision Workshops*, pages 1907–1915.

Yu, B., Liu, T., Gong, M., Ding, C., and Tao, D. (2018). Correcting the triplet selection bias

for triplet loss. In *Proceedings of the European Conference on Computer Vision (ECCV)*, pages 71–87.

Zhang, F., Zhu, X., and Ye, M. (2018). Fast human pose estimation. In *Proceedings of the IEEE/CVF Conference on Computer Vision and Pattern Recognition*, pages 3517–3526.

Zhao, X., Wu, X., Miao, J., Chen, W., Chen, P. C., and Li, Z. (2022). Alike: Accurate and lightweight keypoint detection and descriptor extraction. *IEEE Transactions on Multimedia*.

Zhuang, B., Shen, C., Tan, M., Chen, P., Liu, L., and Reid, I. (2022). Structured binary neural networks for image recognition. *International Journal of Computer Vision*, 130(9):2081–2102.